TRENDS IN SCIENCES 2025; 22(12): 10925
https://doi.org/10.48048/tis.2025.10925
RESEARCH ARTICLE

Activated Carbon from Waste Coffee Grounds for Effective Methylene Blue Removal in Textile Wastewater Treatment

Wa Ode Sitti Ilmawati[1,2], Nurmayasari[1], Diki Purnawati[3], Sholihun[1] and Ari Dwi Nugraheni[1,*]

[1]Department of Physics, Faculty of Mathematics and Natural Sciences, Universitas Gadjah Mada, Yogyakarta 55281, Indonesia
[2]Department of Physics, Faculty of Mathematics and Natural Sciences, Universitas Halu Oleo, Kampus Hijau Bumi Tridharma, Kendari 93232, Indonesia
[3]Research Center for Electronics, National Research and Innovation Agency, Jawa Barat 40135, Indonesia

([*]Corresponding author's e-mail: ari.dwi.n@ugm.ac.id)

Received: 12 June 2025, Revised: 19 July 2025, Accepted: 29 July 2025, Published: 10 September 2025

Abstract

Utilizing waste coffee grounds (WCGs) to produce activated carbon (WCGs-AC) supports sustainable waste management by converting organic waste into value-added materials. This study investigates the optimization of the production process, physicochemical properties, and adsorption performance of activated carbon derived from WCGs. This study pretreated WCGs using hexane and hot water washing methods, followed by carbonization under oxygen-limited conditions. The resulting WCGs-AC exhibited grain sizes ranging from 1.34 to 1,376.00 nm, high specific surface areas (1,304 - 3,405 m^2/g), pore volumes of 1.262 - 4.079 cm^3/g, and average pore radii between 1.936 and 2.397 nm. Functional groups such as amine (N–H), hydroxyl (–OH), and C–O were identified on the WCGs-AC surface. All WCGs-AC samples achieved 100% Methylene Blue (MB) removal, with similar adsorption capacities ranging from 10.20 ± 0.00 to 10.74 ± 0.02 mg/g. The highest-performing adsorbent was obtained using the hot water washing method and carbonization at 550 °C (WZ550), which exhibited an effectively infinite adsorption rate and sustained 100% removal efficiency over 6 reuse cycles. Various kinetic models, including pseudo-1st-order (PFO), pseudo-2nd-order (PSO), Elovich, and Weber-Morris, were applied to describe the adsorption behavior. These findings demonstrate that low-cost and efficient adsorbents can be derived from coffee waste, offering promising potential for dye removal in textile wastewater treatment.

Keywords: Activated carbon, Adsorption, Hexane, Hot water, Methylene blue, Reusability, WCGs

Introduction

Water pollution is increasingly recognized as a serious environmental issue, driven by the continuous discharge of diverse contaminants such as pharmaceutical residues (e.g., ibuprofen), pesticides, heavy metals, and organic dyes into aquatic systems [1-3]. Many sectors, such as textiles, food processing, printing, cosmetics, and medical manufacturing, heavily rely on dyes. Approximately 15% of the dyes used in textile dyeing processes are lost to wastewater. Methylene blue (MB), a widely used synthetic dye, poses significant environmental and health risks [4]. Exposure to excessive MB may cause symptoms such as nausea, vomiting, and neurotoxicity in humans [5]. Several techniques to mitigate MB contamination have been explored, including adsorption, reverse osmosis membranes [6-9], electrocoagulation [10,11], ion exchange [12], photodegradation [13,14], biodegradation [15-18], oxidation [19], and ozonation [20,21]. Adsorption stands out among these techniques due to its simplicity, low operational cost, and eco-friendly nature [22].

Due to its suitability, operational flexibility, ease of design, and affordability, especially when using low-cost and regenerable adsorbents, adsorption is often considered the most attractive method [23]. Various adsorbents such as resins [24], silica [25], biochar,

zeolites, agricultural biomass, carbon nanotubes [26,27], graphene [28,29], chitosan, clays or organoclays [23], alumina [30], Mg-Al layered double hydroxides [31], and hydroxyapatite [32] have been employed for MB adsorption. However, some of these materials are not particularly effective and exhibit low to moderate adsorption capacity for MB due to their limited porosity and functionality, while others are considered high-cost adsorbents.

Among these materials, carbon-based adsorbents offer greater environmental and economic benefits. Owing to their large surface area and favorable surface functionalities, activated carbon (AC) provides high removal efficiency. AC typically contains many hydroxyl and carboxyl groups, aliphatic double bonds, and aromatic structures [26]. Recent research has shifted toward developing low-cost, readily available, renewable, eco-friendly, and effective adsorbents. Agricultural residues such as biomass, olive stones, corn stalks, rice husks, sugarcane bagasse, fruit seeds, nutshells, fruit pulp, bones, and coffee grounds have been explored as potential precursors for activated carbon production [33].

Coffee beans are widely consumed worldwide in the form of brewed coffee. According to the International Coffee Organization (ICO), 10.5 million tons of coffee beans were harvested globally in 2020 - 2021 [34]. Waste products from coffee processing include spent coffee grounds (WCGs), coffee husks, and silver skin. The annual global production of WCGs is estimated at around 6 million tons [35]. Organic compounds such as caffeine, tannins, and chlorogenic acids are present in this waste and can cause environmental pollution if not properly managed [36].

WCGs contain carboxyl, hydroxyl, carbonyl, and other functional groups that can enhance the adsorption and removal of pollutants from water through hydrogen bonding and electrostatic interactions. Additionally, π–π and hydrophobic interactions contribute to removal [37]. Activated carbon derived from WCGs (WCGs-AC) has demonstrated the ability to adsorb various contaminants, including heavy metals, such as lead [38], copper [39], chromium [40,41], nickel [42], arsenic [43], and mercury [44]; dyes, including methylene blue [45], rhodamine B [46], malachite green [47], Congo red [48], crystal violet [49], aniline yellow [50], orange G [51], and methyl orange [52]; antibiotics, such as tetracycline [53], balofloxacin [54], and sulfamethoxazole [55]; other pollutants, including the pesticides carbendazim and linuron [56], fluoride [57], and bisphenol A [58].

The main steps in preparing activated carbon from spent coffee grounds (WCGs-AC) are similar to conventional activated carbon production methods, involving activating a pore-forming agent. Activation can be performed using either chemical or physical agents. Chemical activators vary widely and may include acids, bases, or salts. Common chemical agents used in activated carbon production include acids such as H_3PO_4, H_2SO_4, and HCl; bases such as KOH and NaOH; and salts including $ZnCl_2$, $FeCl_3$, and $CaCl_2$. ZnCl2 is the most widely used activator for biomass-based precursors among these salts. [59-60].

$ZnCl_2$ pretreatment promotes the formation of mesopores and micropores. It acts as a dehydrating agent, facilitating the removal of moisture and volatile compounds from the biomass precursor. Additionally, $ZnCl_2$ catalyzes cellulose, hemicellulose, and lignin thermal degradation. Increasing the carbonization temperature leads to more mesopores and micropores [39]. $ZnCl_2$ enhances the specific surface area, pore volume, and methylene blue (MB) adsorption capacity of activated carbon derived from shaddock peel. $ZnCl_2$-activated carbon made from citrus peel has demonstrated high MB adsorption performance. The $ZnCl_2$ treatment increased porosity by more than 4.54% and improved MB adsorption capacity up to 336 mg/g [61].

In commercial applications of physical activation, the 2nd step involves activation in an oxidizing gas atmosphere, such as steam, carbon dioxide, nitrogen, or a mixture with air, at elevated temperatures ranging from 400 to 900 °C. The 1st step is carbonization (pyrolysis) conducted in an inert atmosphere. Although physical activation is a relatively costly technique for producing activated carbon, it can yield porous carbon structures with strong physical stability. However, this method has several drawbacks, including limited adsorption capacity, high energy consumption, and extended activation times [33]. To address the challenge of excessive energy consumption, activated carbon in this study was synthesized through gas-free carbonization in a relatively short duration, only 10 min. The absence of a gas flow during pore formation was

compensated for by pre-washing the spent coffee grounds with hexane and hot water before activation. This washing step helps remove coffee oils [62] and other impurities [63,64].

In addition to washing and chemical activation, carbonization temperature is also a key factor in determining the properties of activated carbon. Higher carbonization temperatures - 600, 700 and 800 °C - tend to produce activated carbon from spent coffee grounds with larger specific surface areas [65]. However, care must be taken to avoid damaging the carbon microstructure, which could reduce its effectiveness in adsorbing inorganic pollutants. In highly porous materials, adsorption is typically dominated by pore-filling mechanisms, which may result in a loss of specificity and selectivity toward certain adsorbates. Furthermore, elevated carbonization temperatures can lead to the formation of more hydrophobic carbon with fewer surface heteroatoms, which is less favorable for adsorbing organic pollutants that rely on hydrophobic interactions [66].

For practical applications, an effective adsorbent must exhibit high adsorption capacity and environmental sustainability and demonstrate ease of regeneration and reusability. These requirements have driven growing interest in the recyclability and structural stability of synthesized adsorbents [67]. Regeneration and reuse studies are essential for evaluating the long-term performance and feasibility of adsorbents before their application to real environmental samples [68]. The ability of an adsorbent to maintain its performance over multiple cycles is a key factor in advancing adsorption technologies, particularly for sustainable or long-term operations [69]. Once activated carbon becomes saturated or the contaminant concentration reaches the breakthrough threshold, the spent material must be treated to remove the adsorbed pollutants and restore its adsorption functionality. The regeneration of exhausted adsorbents is a critical parameter for commercial applications, as it directly affects the cost-effectiveness and sustainability of the process [70,71].

In a previous study, waste coffee grounds (WCGs) washed with hexane were directly employed for the removal of Methylene Blue (MB), achieving a maximum adsorption capacity of 416.67 mg/g [72]. Both raw WCGs and their activated form (WCGs-AC) exhibited similar functional groups, including amine (N–H), hydroxyl (–OH), and carbonyl (C–O), which contributed to dye adsorption. However, aspects such as the influence of different washing methods and carbonization temperatures, pore characteristics, post-adsorption properties of WCGs-AC, and adsorption kinetics were not previously investigated. In the present study, 2 washing methods were applied to WCGs - using hexane and hot water - before chemical activation with $ZnCl_2$ and subsequent carbonization under oxygen-limited conditions to enhance their physicochemical properties. The novelty of this work lies in the improved synthesis approach and the comprehensive evaluation of pore structure (via BET analysis), functional group transformations before and after MB adsorption (via FTIR), and adsorption kinetics. The resulting WCGs-AC exhibited a high specific surface area, fast adsorption rate, and excellent reusability. The abundant surface area and active binding sites facilitate MB adsorption through diffusion and chemisorption mechanisms, enabling environmentally sustainable regeneration.

Materials and methods

Materials

The WCGs were collected from the pantry of the Department of Physics, Faculty of Mathematics and Natural Sciences, Universitas Gadjah Mada. $ZnCl_2$ supplied by Pudak Scientific, Indonesia, HCl supplied by Smart Lab, Indonesia, and MB ($C_{16}H_{18}ClN_3S{\cdot}3H_2O$, MW: 373.90 g/mol) provided by Sigma Aldrich.

Fabrication of adsorbent

The fabrication of the adsorbent was conducted according to the experimental scheme shown in **Figure 1**. The WCGs were dried in an oven at 100 °C for 7 h and then stored in a desiccator. The dried WCGs were washed several times with hot water until the washing water became colorless. WCGs were dried in an oven at 100 °C for 7 h. Another washing method for WCGs followed the procedure reported by Nurmayasari *et al.* [72]. First, the WCGs were washed with hexane at a ratio of 1:10 (g/mL) and stirred using a magnetic stirrer at 750 rpm for 2 h. The WCGs were then filtered and washed with 70% ethanol. Finally, the WCGs were rinsed with distilled water until the rinsing water became colorless and then dried.

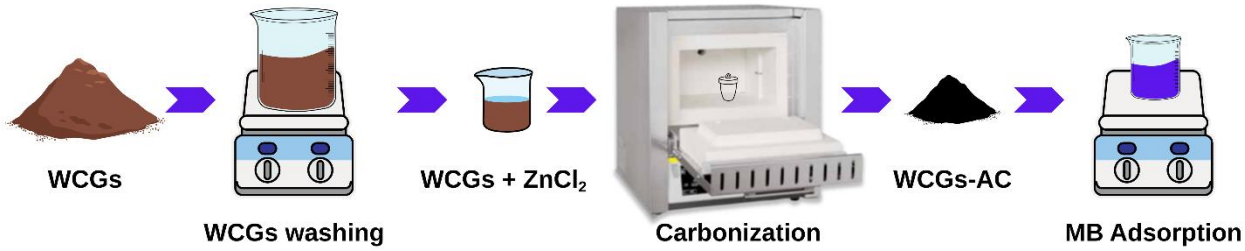

Figure 1 Experimental schematic.

A total of 20 g of the cleaned WCGs were soaked in a solution containing 9 g of $ZnCl_2$ in 60 mL of water for 24 h. The WCGs were then dried at 100 °C for 5 h. The activated WCGs were subsequently carbonized at 450, 500 and 550 °C for 10 min in a furnace (heating rate: 5 °C/min), cooled to room temperature in air, and neutralized with 50 mL of 5% HCl for 2 h. They were then rinsed with distilled water several times until the pH of the rinsing water was neutral. The WCGs-AC were sieved using a 200-mesh sieve to achieve uniform particle size. Then WCGs-AC was stored in a desiccator before characterization and adsorption experiments. The resulting WCGs-AC samples were named according to their washing methods and carbonization temperatures, as shown in **Table 1**.

Table 1 WCGs-AC adsorbents in this study.

WCGs-AC	Washing Method	Carbonization temperature (°C)
WZ450	hot water	450 ± 1
WZ500	hot water	500 ± 1
WZ550	hot water	550 ± 1
HZ450	hexane	450 ± 1
HZ500	hexane	500 ± 1
HZ550	hexane	550 ± 1

Characteristics of the adsorbent

WCGs-AC were characterized using a Particle Size Analyzer (PSA), Brunauer-Emmett-Teller (BET) analysis, Scanning Electron Microscopy (SEM), and Fourier Transform Infrared Spectroscopy (FTIR). The PSA was used to determine the particle size distribution of the material. The BET technique was applied to analyze the specific surface area, total pore volume, and size distribution. SEM imaging was conducted to investigate the microstructure and morphology of the activated coffee grounds at the micro/nano scale and to assess the elemental composition of the material quantitatively. FTIR analysis was conducted to characterize the functional groups on the adsorbent surface. FTIR measurements were performed using the KBr pellet method in the wavenumber range of 400 - 4,000 cm^{-1} at room temperature. The FTIR spectra provide absorbance profiles indicating the functional groups of the sample. The absorption peaks observed in the spectra were compared with standard reference data to identify the types of functional groups present.

The particle size distribution was analyzed using a Microtrac Flex 11.106. The BET surface characteristics and porosity of the WCGs-AC were measured using a QuantaTec 11.06 instrument. Surface morphology and elemental composition of WCGs-AC before and after adsorption were examined using a scanning electron microscope equipped with energy-dispersive X-ray spectroscopy (SEM/EDX, JEOL JSM-6510). Diffraction patterns were collected using a Bruker D8 Advance Eco X-ray diffraction (XRD) system. FTIR spectra (Thermo Nicolet iS10) of WCGs-AC before and after adsorption were also analyzed to investigate the adsorption mechanisms.

Batch experiments

A 10 ppm MB solution was treated with WCGs-AC adsorbents listed in **Table 1**, each applied at 1 g/L. The WCGs-AC was stirred in the MB solution at 500

rpm for 10 to 60 min at room temperature. At 10-min intervals, the absorbance of the aliquots was recorded at 664 nm using a UV-Vis spectrophotometer. The adsorption capacity (q_e) and MB removal efficiency (R) of the WCGs-AC were calculated using Eqs. (1) and (2).

$$q_e = (C_0 - C_e)V/m \quad (1)$$

$$R = [(C_0 - C_e)/C_0] \times 100\% \quad (2)$$

q_e (mg/g) is the adsorption capacity, C_0 (mg/L) is the initial MB concentration, and C_e is the MB concentration at equilibrium, V (L) is the MB volume, m (g) is the WCGs-AC mass, and R (%) is the removal efficiency.

The pseudo-1st-order, pseudo-2nd-order, Elovich, and Weber-Morris models fit the time series experimental data [73]. The models are described in Eqs. (3) - (9).

Pseudo-1st order (PFO) model: non-linear $q_t = q_e(1 - e^{-k_1 t})$ (3)

Linear: $ln\ ln\ (q_e - q_t) = ln\ ln\ q_e - k_1 t$ (4)

Pseudo-2nd order (PSO) model: non-linear $q_t = k_2 q_e^2 t/(1 + k_2 q_e t)$ (5)

Linear: $1/q_t = 1/k_2 q_e^2 t + 1/q_e$ (6)

Elovich model: non-linear $dq_t/dt = ae^{-bq_t}$ (7)

Linear: $q_t = (1/b)\ ln\ ln\ (ab) + (1/b)\ ln\ ln\ (t)$ (8)

Weber-Morris model: $q_t = k_{WM} t^{\frac{1}{2}} + C$ (9)

q_t (mg/g) denotes the quantity of adsorbate adsorbed at time t (m), k_1 (/m) is the rate constant of the pseudo-1st-order equation, k_2 (L/mg m) is the rate constant of the pseudo-2nd-order equation, a is the initial adsorption rate constant of the Elovich model (mg/g h), b is the desorption rate constant of the Elovich model (g/mg), k_{WM} (mg/g $m^{0,5}$) is the rate constant of the intraparticle equation, and C is the linear intercept.

WCGs-AC 1.00 g/L had been tested for MB adsorption for 60 min and showed a MB degradation percentage of 100%. Repeated adsorbent testing was carried out up to 10 cycles. **Table 2** summarizes the preparation methods, pore characteristics, and kinetic performance of various activated carbon-based adsorbents for methylene blue removal, providing a comparison for this study.

Table 2 Preparation, pore properties, and kinetics performance of different AC-based adsorbents used for MB removal.

Adsorbent types	Washing method and carbonization temperature	Pore properties			Kinetic performance			Removal (%)	No. of cycle	Ref.
		S_{BET}	V_t	d_p	q_e	k_2	R^2			
		m^2/g	cm^3/g	nm	mg/g	g/mg min				
WCGs/KOH	800 °C	1,199	0.42	-	106.38	2231.65	0.9995	-	-	[45]
Commercial	-	833	2.5	-	100.38	2179.47	0.9873	-	-	[45]
WCGs	500 °C	-	-	-	5.8959	0.0547	0.9827	-	-	[74]
WCGs/ H_3PO_4	WCGs boiled in DW* 3 times, 600 °C	-	-	-	25.19	0.003	0.9958	77.8	3	[75]
WCGs/$ZnCl_2$	WCGs boiled in DW* 3 times, 600 °C	-	-	-	42.92	0.001	0.9921	78.9	3	[75]
WCGs/NaOH	WCGs are washed with NaOH, 300 °C	-	-	-	142.8	3.7×10^{-4}	0.932	-	-	[76]
WCGs/H_3PO_4+P_4O_{10}	DW* washing	662.4	0.377	< 2	101.17	9.4×10^{-7}	0.9905	52.4	6	[77]

*rT: room temperature

Results and discussion

Grain size of adsorbents

The dominant particle size distribution of WCGs-AC, as measured using a Particle Size Analyzer (PSA), is shown in **Table 3**. A comparison between WCGs-AC washed with hot water (WZ) and those washed with hexane (HZ) reveals that WZ exhibits a larger particle size than HZ. These findings imply that the hot water

washing process leads to greater particle agglomeration than hexane washing. The increase in carbonization temperature resulted in a corresponding particle size enlargement, presumably due to intensified structural reorganization and material densification during thermal processing. Furthermore, the WCGs-AC samples washed with hot water exhibited larger particle sizes than those treated with hexane, indicating that the washing medium exerts a distinct influence on particle aggregation behavior. Although larger particle sizes tend to exhibit higher adsorption kinetic rates, particle size has a negligible effect on the adsorption capacity at equilibrium. In contrast, previous studies have reported that smaller particle sizes enhance adsorption capacity due to the increased surface area and shorter diffusion pathways [78].

Table 3 The **particle size distribution** of WCGs-AC

WCGs-AC	Diameter (nm)
WZ450	368.00
WZ500	471.00
WZ550	1376.00
HZ450	1.34
HZ500	432.00
HZ550	643.00

Surface area, pore volume, and pore size of adsorbents

The surface area, pore volume, and pore size of WCGs-AC are summarized in **Table 4**. The material exhibits relatively high surface area and pore volume, with surface area values ranging from 1,304 to 3,450 m^2/g, which are considered exceptionally high. According to Hou *et al.* [79], such values fall into the "super high" classification. Compared with commercial adsorbents and adsorbents produced by other researchers in **Table 2**, the commercial adsorbents and those in this study have the highest surface area and pore volume. Based on IUPAC pore size classification, WCGs-AC in this study is categorized as mesoporous, with pore diameters between 2 and 50 nm [80]. Mesopores provide a large surface area, significantly enhancing the adsorption capacity of WCGs-AC [39]. A comparison of different WCG washing methods revealed that WCGs-AC washed with hot water had a higher surface area than those washed with hexane. However, Zhao (2022) reported that WCGs washed with hot water showed a much lower surface area (0.6744 m^2/g), total pore volume (6.1×10^{-5} cm^3/g), and average pore diameter (2.126 nm), which is still within the mesoporous range [81]. In contrast, the current study indicates that hot water washing did not significantly influence the pore characteristics of WCGs-AC. Therefore, it can be reasonably concluded that $ZnCl_2$ activation and carbonization temperature are the dominant factors affecting the pore structure of WCGs-AC.

The specific surface area (S_{BET}), total pore volume (V_T), and average pore diameter (D) of WCGs-AC tend to decrease with increasing carbonization temperature, regardless of whether the samples were washed with hot water or hexane. Notably, WCGs-AC washed with hexane exhibited a more pronounced decline. The reductions in SBET and VT suggest the occurrence of pore degradation. Using WZ450 as a reference, the pore degradation observed in WZ500 and WZ550 was 19.59% and 12.53%, respectively. For the hexane-washed samples, pore degradation increased progressively with temperature. Compared to HZ450, HZ500 showed a 7.62% decrease, while a substantial degradation of 56.47% was observed in HZ550.

During the impregnation and carbonization processes, WCGs-AC undergoes pore formation, pore enlargement, and pore degradation [82]. At 450 °C, the rate of pore formation exceeds that of enlargement and degradation, resulting in higher surface area and pore

volume. However, at 500 and 550 °C, the pore enlargement and degradation rates become dominant, leading to a net loss in pore structure. Consequently, this degradation contributes to decreased pore volume and surface area.

Table 4 WCGs-AC surface area, pore volume, and pore size.

WCGs-AC	Surface area (m^2/g)	Pore volume (cm^3/g)	Average pore radius (nm)
WZ450	3405	4.079	2.396
WZ500	2792	3.280	2.350
WZ550	2977	3.568	2.397
HZ450	2382	2.899	2.434
HZ500	2302	2.678	2.327
HZ550	1304	1.262	1.936

The consistency between BET and PSA analyses reinforces the interpretation of the mesoporous structure's role in enhancing adsorption. Despite the increase in particle size at higher carbonization temperatures, surface area may decline due to structural densification and pore degradation. A trade-off exists between particle size and surface area, which are crucial for maximizing adsorption efficiency. The high specific surface area of the activated carbon likely enhances its adsorption capacity by providing more active sites for dye molecules to interact with the adsorbent surface [50].

WCGs-AC morphology

SEM images indicate that pore structures begin to form following hot water and hexane washing, as shown in **Figure 2**. Hot water-washed WCGs show a higher density of open pores, highlighting the effectiveness of this pretreatment method. Pretreatment with hot water appears more effective in promoting porosity compared to hexane.

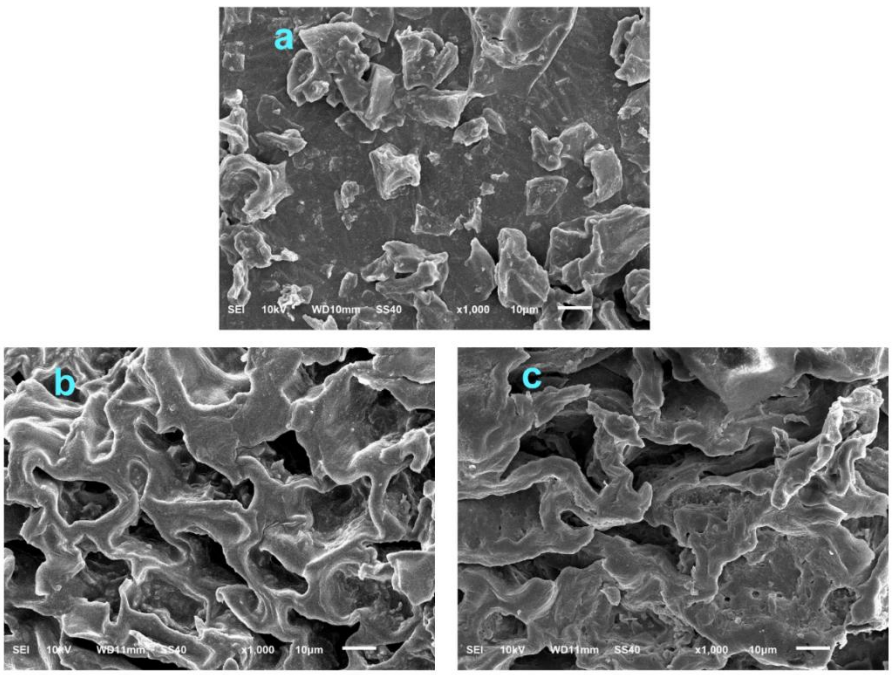

Figure 2 WCGs are (a) before washing, (b) washed with hot water, and (c) with hexane.

WCGs-AC exhibits an irregular and heterogeneous surface morphology characterized by pores of various shapes and sizes, as shown in **Figure 3**. A comparison of WCGs-AC samples reveals that WZ exhibits larger and more numerous pores than HZ. This observation is consistent with the BET analysis, confirming that WZ-derived WCGs-AC has a greater total surface area and pore volume than HZ-derived WCGs-AC. The effect of carbonization temperature on surface morphology is evident when comparing the 2 columns in **Figure 3**. As the carbonization temperature increases, both the size and number of pores tend to decrease, resulting in a reduced total surface area, as indicated by the BET results. This suggests that although higher temperatures promote carbon structure development, excessive carbonization may lead to pore shrinkage or collapse, reducing the number of available adsorption sites.

SEM images confirm the porous nature of the WCGs-AC, while BET analysis indicates an average pore radius ranging between 1.936 and 2.434 nm. Considering the molecular size of MB (1.382 - 1.447 nm in length and ~0.95 nm in width [74], it is likely that the pores of WCGs-AC provide sufficient space for adsorption.

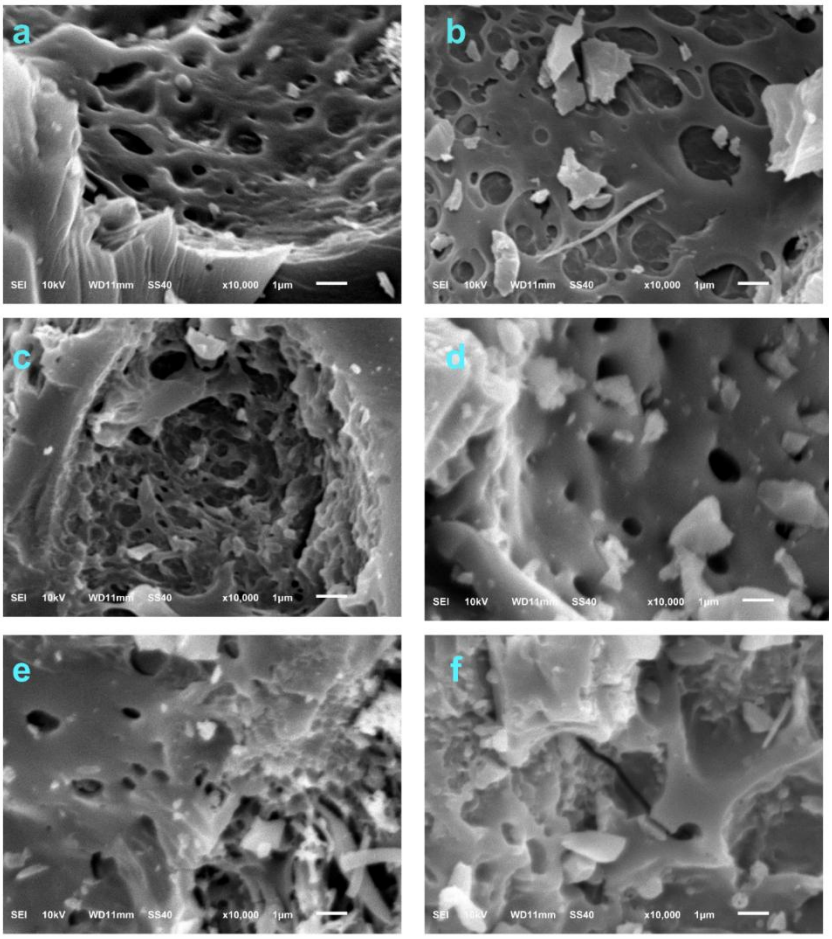

Figure 3 SEM image of WCGs-AC: (a) WZ450, (b) WZ500, (c) WZ550, (d) HZ450, (e) HZ500, (f) HZ550.

WCGs-AC functional groups before and after MB adsorption

Figure 4 presents the FTIR spectra of WCGs-AC washed with hexane (HZ550) and hot water (WZ550). Functional groups identified include hydroxyl (–OH), amine (N–H), methylene (C–H), and carbonyl (C–O), which contain electronegative atoms (O, H, and N) capable of interacting with corresponding atoms in methylene blue (MB) molecules [74]. The characteristic bands of –OH and N–H stretching (3,100 - 3,600 cm^{-1}), C–H (2,924, 2,854, 1,465 and 1,381 cm^{-1}), C≡C (2,368 and 2,337 cm^{-1}), C=C (1,566 cm^{-1}), and C–O (1126 cm^{-1}) exhibited similar intensities in both samples, except for the C≡C band, which was more pronounced

in HZ550, suggesting a higher concentration of this group. These findings indicate that the washing method had minimal influence on the surface functional groups of WCGs-AC. F**igure 5** illustrates the impact of carbonization temperature on the functional groups of WCGs-AC. All samples displayed the presence of –OH, N–H, C–H, C≡C, C=C, C–O, and aromatic structures, with varying intensities. Among them, WZ550 exhibited the highest overall band intensities, indicating a richer surface chemistry. Accordingly, 550 °C was identified as the optimal carbonization temperature in this study.

Following MB adsorption, a marked increase in the –OH band intensity was observed, indicating the formation of strong covalent or ionic interactions between –OH groups on WCGs-AC and MB molecules (**Figure 6**). The C=C band shifted from 1,566 to 1,627 cm^{-1}, while the C–H bands at 1,465 and 1,381 cm^{-1} intensified. New absorption bands also emerged corresponding to N–O (1,319 cm^{-1}) and C–N (1242 cm^{-1}). The shift and new groups may occur due to hydrogen bonding in WCGs-AC with nitrogen or other atoms in MB. Additionally, aromatic C–H (825, 810, and 756 cm^{-1}) and C=C (694 and 678 cm^{-1}) groups present in WCGs-AC are associated with π-electron systems that can engage in π–π stacking interactions with the aromatic rings of MB, thereby enhancing the adsorption capacity [74]. The appearance of additional aromatic peaks at 871, 794, and 678 cm^{-1} after MB adsorption further supports this mechanism.

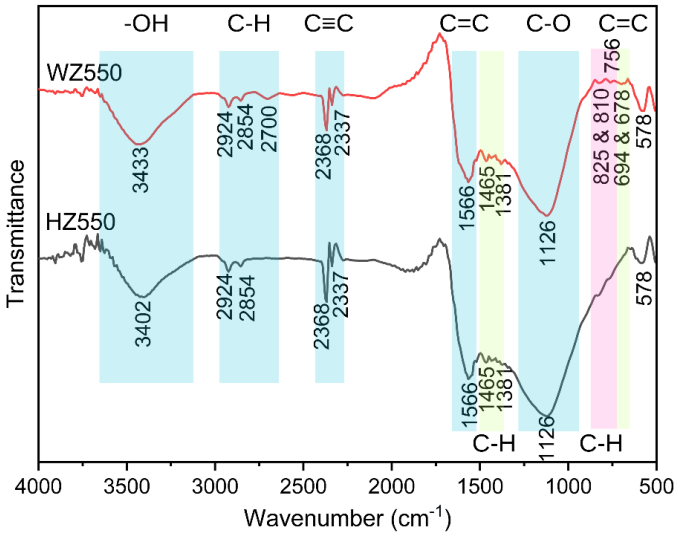

Figure 4 WCGs-AC washing comparison.

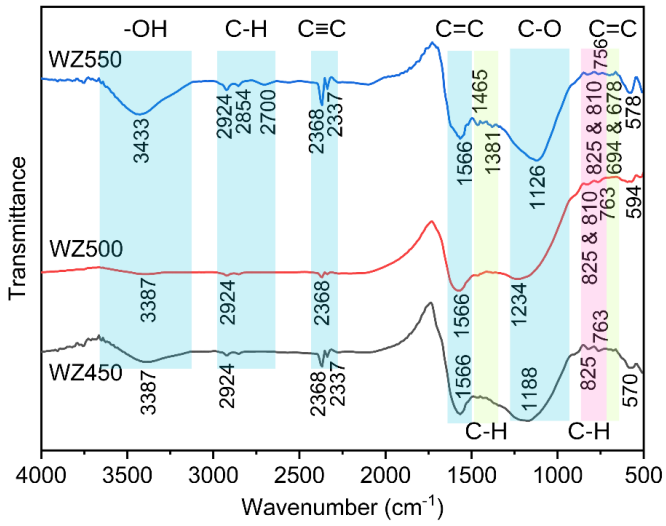

Figure 5 WCGs-AC carbonization temperature comparison.

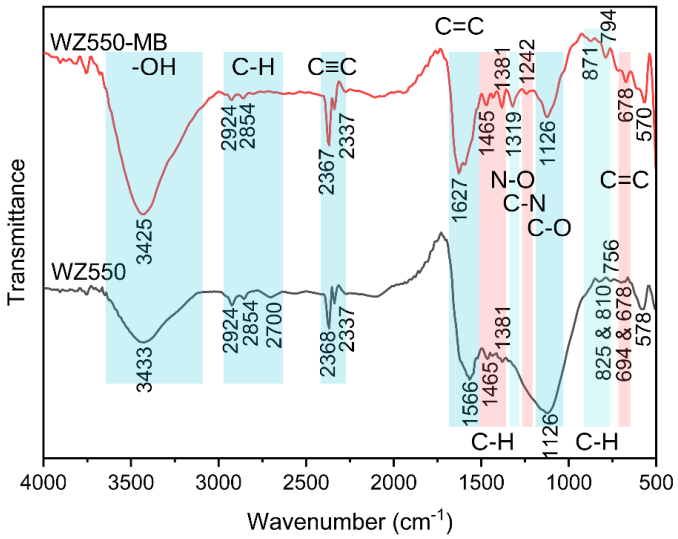

Figure 6 WZ550 before and after MB adsorption.

Characteristic and kinetic comparison study

The kinetic data reveal that the adsorption of MB onto WCGs-AC is best fitted by the PSO model, indicating that chemisorption is the dominant mechanism [78]. This is further supported by FTIR analysis, which confirms the involvement of chemical interactions. The coefficients of determination (R^2) for the kinetic models are summarized in **Table 5**. In contrast, HZ450 and HZ500 exhibited good fits with the PFO and PSO models, suggesting a mixed mechanism involving physisorption and chemisorption [83]. The experimentally determined adsorption capacity ($q_{e,exp}$) for WCGs-AC is 10.20 mg/g, while the theoretical kinetic parameters are listed in **Table 6**. Pretreatment with hot water and higher carbonization temperatures enhances the adsorption rate, as evidenced by increased k_1 and k_2 values. WZ550 exhibited the highest rate constant among all samples, indicating superior adsorption kinetics. These findings suggest a synergistic effect between the pretreatment method and thermal processing in improving adsorption performance.

Table 5 Regression of determination (R^2) of WCGs-AC kinetic models.

WCGs-AC	R^2			
	PFO	**PSO**	**Elovich**	**Weber-Morris**
WZ450	-	0.9999	0.6572	0.6906
WZ500	-	0.9999	0.6572	0.6602
WZ550	-	1.0000	-	0.6590
HZ450	0.9785	0.9979	0.7557	0.8079
HZ500	0.9830	0.9999	0.7415	0.6839
HZ550	-	0.9999	0.6572	0.6833

Table 6 Kinetic parameters of triplication MB adsorption on WCGs-AC.

WCGs-AC	k_1 (/min)	$q_{e\text{-kinetic theory}}$ (mg/g)	k_2 (g/mg min)	$q_{e\text{-kinetic theory}}$ (mg/g)
WZ450	-	-	0.29 ± 0.033	$10.27 \pm 8.537\times10^{-3}$
WZ500	-	-	8.6 ± 1.4	$10.20 \pm 4.408\times10^{-4}$
WZ550	-	-	infinite	10.20 ± 0
HZ450	0.206 ± 0.00752	14.1 ± 0.860	0.0364 ± 0.00132	$10.74 \pm 1.958\times10^{-2}$
HZ500	0.274 ± 0.00629	8.30 ± 0.259	0.347 ± 0.00419	$10.26 \pm 8.652\times10^{-4}$
HZ550	-	-	0.390 ± 0.00592	$10.25 \pm 8.270\times10^{-4}$

The kinetic parameters obtained in this study are compared with those reported in previous studies (**Table 2**), with WZ550 representing the current findings due to its superior performance. Although the q_e of WZ550 is relatively lower than that reported in some studies, its k_2 is extremely high. Furthermore, the PSO model provides an excellent fit to the experimental data for WZ550, with an R^2 of 1.0.

Adsorbents reusability

WZ500 retained its adsorption capacity over 6 cycles, indicating superior structural resilience. Compared to HZ500, WZ500 shows extended usability with minimal decline in performance over time (**Figure 7(a)**). Thermal activation appears to strengthen the adsorbent matrix, contributing to enhanced reusability. WZ450 maintained full adsorption efficiency for 4 cycles, WZ500 for 6 cycles, and WZ550 for 7 cycles (**Figure 7(b)**). This study demonstrates the importance of thermal treatment in developing regenerable adsorbents for wastewater treatment.

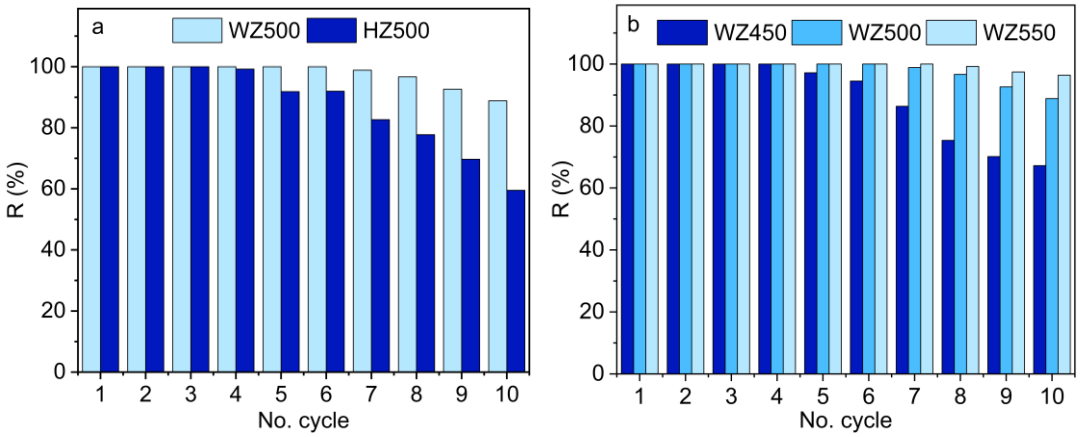

Figure 7 The reusability of WCGs-AC is influenced by (a) washing methods and (b) carbonization temperatures.

Table 2 compares the reusability study conditions and results of various AC-based adsorbents used for MB removal. Due to differences in adsorption, desorption, and regeneration parameters, the reusability performance varied significantly among the adsorbents. The WCGs-AC developed in this study sustained a high removal efficiency over 10 regeneration cycles. Particularly, WZ550 maintained a removal efficiency of 96.39 ± 0.01 % in the tenth cycle, indicating excellent reusability.

Limitations and future work

Despite the promising performance of WCGs-AC, several limitations should be acknowledged. First, there is a potential risk of leaching of residual $ZnCl_2$ or its transformation products (e.g., ZnO) into aqueous environments [84], even after post-treatment washing.

Trace amounts of Zn may still be released under varying pH and ionic strength conditions, potentially contributing to secondary contamination [85]. Second, the thermal treatment employed in this study involved a short carbonization time (10 min) under ambient atmospheric conditions. These parameters may lead to incomplete carbonization, limited pore development, and partial oxidation due to the presence of atmospheric oxygen [86], thereby compromising the structural quality of the resulting material [87]. Third, the adsorbent's performance was evaluated only under controlled laboratory conditions using synthetic methylene blue solutions. However, real wastewater typically contains a complex matrix of competing ions and organic substances, which may interfere with the adsorption process and reduce the overall efficiency [88].

To address these limitations and enhance the environmental sustainability of the material, future studies should include systematic Zn leaching assessments under diverse water chemistries and explore optimized washing or recycling protocols to minimize metal release [85]. The carbonization process should be refined by employing inert gas atmospheres (e.g., nitrogen or argon) and extending residence time to improve the physicochemical properties and reproducibility of the adsorbent [87]. Furthermore, adsorption experiments should be conducted using actual wastewater samples to evaluate the material's practical applicability and robustness under realistic treatment conditions [88]. Alternative green activation strategies, such as phosphoric acid (H_3PO_4), offer a promising substitute for $ZnCl_2$, as they eliminate the need for inert atmospheres and reduce environmental impacts while maintaining high surface area and adsorption performance [89]. Additionally, the integration of environmentally friendly technologies, such as the Continuous Submerged Solid Small-Scale Laboratory Photoreactor (CS4PR) employing TiO_2/NO_3^- catalysts, may further support sustainable wastewater treatment approaches [90]. Finally, the multipollutant adsorption capacity of WCGs-AC - including for heavy metals, dyes, and pharmaceutical compounds - should be further explored to validate its potential as a versatile and cost-effective adsorbent for diverse water treatment applications [91].

Conclusions

WCGs-AC synthesized using the method proposed in this study exhibited a micro- to nano-scale grain size, non-uniform surface morphology, a large specific surface area, and the presence of amine, hydroxyl, and C–O functional groups, which serve as active sites for MB adsorption. The adsorption mechanism was predominantly governed by covalent interactions and π–π bonding. The PSO model best described the adsorption kinetics, with kinetic capacities ranging from 10.20 ± 0.00 to 10.74 ± 0.02 mg/g. The WZ550 adsorbent demonstrated an infinite adsorption rate and maintained 100% removal efficiency over 6 consecutive reuse cycles. Its consistent performance across multiple cycles highlights its potential for practical application in industrial-scale wastewater treatment.

Acknowledgements

Indonesian Education Scholarship (BPI), Center for Higher Education Funding and Assessment (PPAPT), Ministry of Higher Education, Science, and Technology of the Republic of Indonesia, Indonesia Endowment Fund for Education (LPDP) have funded/sponsored the implementation of this work.

Declaration of Generative AI in Scientific Writing

The authors acknowledge the use of generative AI tools (e.g., Grammarly and ChatGPT by OpenAI) during the preparation for language editing and grammar correction. No content generation or data interpretation was carried out by AI. The authors take full responsibility for the content and conclusions presented in this work.

CRediT Author Statement

Wa Ode Sitti Ilmawati: Methodology, Data curation, Data analysis, Investigation, Funding acquisition, and Writing –original draft.

Nurmayasari: Data curation, Data analysis, and Investigation.

Diki Purnawati: Resources, Data analysis, and Investigation.

Sholihun: Conceptualization, Software, and Writing – review & editing.

Ari Dwi Nugraheni: Conceptualization, Methodology, Resources, and Supervision.

References

[1] I Ali, P Singh, HYA -Enein and B Sharma. Chiral analysis of ibuprofen residues in water and sediment. *Analytical Letters* 2009; **42(2)**, 1747-1760.

[2] AA Basheer. Chemical chiral pollution: Impact on the society and science and need of the regulations in the 21st century. *Chirality* 2018; **30(4)**, 402-406.

[3] AA Basheer and I Ali. Stereoselective uptake and degradation of (±)-o,p-DDD pesticide stereomers in water-sediment system. *Chirality* 2018; **30(9)**, 1088-1095.

[4] S Karoui, RB Arfi, K Mougin, A Ghorbal, AA Assadi and A Amrane. Synthesis of novel biocomposite powder for simultaneous removal of hazardous ciprofloxacin and methylene blue: Central composite design, kinetic and isotherm studies using Brouers-Sotolongo family models. *Journal of Hazardous Materials* 2020; **387**, 121675.

[5] ZH Mussa, LR Al-Ameer, FF Al-Qaim, IF Deyab, H Kamyab and S Chelliapan. A comprehensive review on adsorption of methylene blue dye using leaf waste as a bio-sorbent: Isotherm adsorption, kinetics, and thermodynamics studies. *Environmental Monitoring and Assessment* 2023; **195(8)**, 940.

[6] RS Bangari, A Yadav, J Bharadwaj and N Sinha. Boron nitride nanosheets incorporated polyvinylidene fluoride mixed matrix membranes for removal of methylene blue from aqueous stream. *Journal of Environmental Chemical Engineering* 2022; **10(1)**, 107052.

[7] A Ulu, M Alpaslan, A Gultek and B Ates. Eco-friendly chitosan/κ-carrageenan membranes reinforced with activated bentonite for adsorption of methylene blue. *Materials Chemistry and Physics* 2022; **278**, 125611.

[8] SS Vedula and GD Yadav. Wastewater treatment containing methylene blue dye as pollutant using adsorption by chitosan lignin membrane: Development of membrane, characterization and kinetics of adsorption. *Journal of the Indian Chemical Society* 2022; **99(1)**, 100263.

[9] H Raval, R Sharma and A Srivastava. Novel protocol for fouling detection of reverse osmosis membrane based on methylene blue colorimetric method by image processing technique. *Water Science and Technology* 2024; **89(3)**, 513-528.

[10] A Hasnaoui, M Chikhi, F Balaska, W Seraghni, M Boussemghoune and N Dizge. Electrocoagulation employing recycled aluminum electrodes for methylene blue remediation. *Desalination and Water Treatment* 2024; **319(42)**, 100453.

[11] G Somasundaram, T Thavamani and S Thangavelu. Integration of sequential electrocoagulation and adsorption for effective removal of colour and total organic carbon in textile effluents and its utilization for seed germination and irrigation. *Environmental Science and Pollution Research* 2024; **31(21)**, 30716-30734.

[12] IM Minisy, NA Salahuddin and MM Ayad. Adsorption of methylene blue onto chitosan-montmorillonite/polyaniline nanocomposite. *Applied Clay Science* 2021; **203(22)**, 105993.

[13] Y Guo, X Fu, R Liu, M Chu and W Tian. Efficient green photocatalyst of Ag/ZnO nanoparticles for methylene blue photodegradation. *Journal of Materials Science: Materials in Electronics* 2022; **33(5)**, 1-13.

[14] EHA Zaid, JC Sin, SM Lam and AR Mohamed. Fabrication of La, Ce co-doped ZnO nanorods for improving photodegradation of methylene blue. *Journal of Rare Earths* 2024; **42(1)**, 76-83.

[15] M Aravind, A Ahmad, I Ahmad, M Amalanathan, K Naseem, SMM Mary, C Parvathiraja, S Hussain, TS Algarni, M Pervaiz and M Zuber. Critical green routing synthesis of silver NPs using jasmine flower extract for biological activities and photocatalytical degradation of methylene blue. *Journal of Environmental Chemical Engineering* 2021; **9(1)**, 104877.

[16] FE Koc and TG Altıncekic. Investigation of gelatin/chitosan as potential biodegradable polymer films on swelling behavior and methylene blue release kinetics. *Polymer Bulletin* 2021; **78(2)**, 3383-3398.

[17] K Wu, M Shi, X Pan, J Zhang, X Zhang, T Shen and Y Tian. Decolourization and biodegradation of methylene blue dye by a ligninolytic enzyme-producing Bacillus thuringiensis: Degradation products and pathway. *Enzyme and Microbial Technology* 2022; **156**, 109999.

[18] KE Abbadi, F Echabbi, Y Ouzidan, AK Idrissi, R Lakhmiri and M Safi. The study on the use of a biocatalyst based on Calcined Cow Teeth-TiO_2 composite in degrading the methylene blue dye. *Results in Chemistry* 2023; **6(1)**, 101027.

[19] X Dong, Y Lin, G Ren, Y Ma and L Zhao. Catalytic degradation of methylene blue by fenton-like oxidation of ce-doped MOF. *Colloids and Surfaces A: Physicochemical and Engineering Aspects* 2021; **608**, 125578.

[20] M Babar, HMS Munir, A Nawaz, N Ramzan, U Azhar, M Sagir, MS Tahir, A Ikhlaq, SNHM Azmin, M Mubashir, KS Khoo and KW Chew. Comparative study of ozonation and ozonation catalyzed by Fe-loaded biochar as catalyst to remove methylene blue from aqueous solution. *Chemosphere* 2022; **307(P1)**, 135738.

[21] F Javed, A Tariq, A Ikhlaq, OS Rizvi, U Ikhlaq, UY Qazi and F Qi. Application of laboratory-grade recycled borosilicate glass coated with iron and cobalt for the removal of methylene blue by catalytic ozonation process. *Arabian Journal for Science and Engineering* 2023; **48**, 8753-8768.

[22] KO Iwuozor, JO Ighalo, LA Ogunfowora, AG Adeniyi and CA Igwegbe. An empirical literature analysis of adsorbent performance for methylene blue uptake from aqueous media. *Journal of Environmental Chemical Engineering* 2021; **9(4)**, 105658.

[23] P Kaur, Kalpana, S Kumar, A Kumar and A Kumar. Effect of various sodium hydroxide treatment parameters on the adsorption efficiency of rice husk for removal of methylene blue from water. *Emergent Materials* 2023; **6(10)**, 1809-1824.

[24] R Coşkun, S Savcı and A Delibaş. Fast removal of methylene blue (MB) with functionalized resin. *Journal of Macromolecular Science Part A* 2019; **56(7)**, 1-11.

[25] EC Peres, JC Slaviero, AM Cunha, AH Bandegharaei and GL Dotto. Microwave synthesis of silica nanoparticles and its application for methylene blue adsorption. *Journal of Environmental Chemical Engineering* 2018; **6(1)**, 649-659.

[26] PO Oladoye, TO Ajiboye, EO Omotola and OJ Oyewola. Methylene blue dye: Toxicity and potential elimination technology from wastewater. *Results in Engineering* 2022; **16(6)**, 100678.

[27] ZA ALOthman, AY Badjah and I Ali. Facile synthesis and characterization of multi walled carbon nanotubes for fast and effective removal of 4-tert-octylphenol endocrine disruptor in water. *Journal of Molecular Liquids* 2019; **275(12)**, 41-48.

[28] T Liu, Y Li, Q Du, J Sun, Y Jiao, G Yang, Z Wang, Y Xia, W Zhang, K Wang, H Zhu and D Wu. Adsorption of methylene blue from aqueous solution by graphene. *Colloids and Surfaces B: Biointerfaces* 2012; **90(1)**, 197-203.

[29] I Ali, AV Babkin, IV Burakova, AE Burakov, EA Neskoromnaya, AG Tkachev, S Panglisch, N AlMasoud and TS Alomar. Fast removal of samarium ions in water on highly efficient nanocomposite-based graphene oxide modified with polyhydroquinone: Isotherms, kinetics, thermodynamics and desorption. *Journal of Molecular Liquids* 2021; **329(2)**, 115584.

[30] S Ali, Y Abbas, Z Zuhra and IS Butler. Synthesis of γ-alumina (Al_2O_3) nanoparticles and their potential for use as an adsorbent in the removal of methylene blue dye from industrial wastewater. *Nanoscale Advances* 2019; **1(1)**, 213-218.

[31] X Pan, M Zhang, H Liu, S Ouyang, N Ding and P Zhang. Adsorption behavior and mechanism of acid orange 7 and methylene blue on self-assembled three-dimensional MgAl layered double hydroxide: Experimental and DFT investigation. *Applied Surface Science* 2020; **522**, 146370.

[32] M Aaddouz, K Azzaoui, N Akartasse, E Mejdoubi, B Hammouti, M Taleb, R Sabbahi and SF Alshahateet. Removal of methylene blue from aqueous solution by adsorption onto hydroxyapatite nanoparticles. *Journal of Molecular Structure* 2023; **1288**, 135807.

[33] S Husien, RM El-taweel, AI Salim, IS Fahim, LA Said and AG Radwan. Review of activated carbon adsorbent material for textile dyes removal: Preparation, and modelling. *Current Research in Green and Sustainable Chemistry* 2022; **5(1)**, 100325.

[34] MRD Silva, FS Bragagnolo, RL Carneiro, IOC Pereira, JAA Ribeiro, CM Rodrigues, RE Jelley, B

Fedrizzi and CS Funari. Metabolite characterization of fifteen by-products of the coffee production chain: From farm to factory. *Food Chemistry* 2022; **369**, 130753.

[35] KT Lee, YT Shih, S Rajendran, YK Park and WH Chen. Spent coffee ground torrefaction for waste remediation and valorization. *Environmental Pollution* 2023; **324**, 121330.

[36] C Setter, FA Borges, CR Cardoso, RF Mendes and TJP Oliveira. Energy quality of pellets produced from coffee residue: Characterization of the products obtained via slow pyrolysis. *Industrial Crops and Products* 2020; **154**, 112731.

[37] LL Kang, YN Zeng, YT Wang, JG Li, FP Wang, YJ Wang, Q Yu, XM Wang, R Ji, D Gao and Z Fang. Removal of pollutants from wastewater using coffee waste as adsorbent: A review. *Journal of Water Process Engineering* 2022; **49**, 103178.

[38] JG Kim, HB Kim and K Baek. Novel electrochemical method to activate biochar derived from spent coffee grounds for enhanced adsorption of lead (Pb). *Science of The Total Environment* 2023; **886**, 163891.

[39] SS Choi, TR Choi and HJ Choi. Surface modification of phosphoric acid-activated carbon in spent coffee grounds to enhance Cu (II) adsorption from aqueous solutions. *Applied Chemistry for Engineering* 2021; **85(4)**, 1218-1234.

[40] R Campbell, B Xiao and C Mangwandi. Production of activated carbon from spent coffee grounds (SCG) for removal of hexavalent chromium from synthetic wastewater solutions. *Journal of Environmental Management* 2024; **366(7)**, 121682.

[41] I Loulidi, F Boukhlifi, M Ouchabi, A Amar, M Jabri, A Kali and F Aziz. Kinetic. Isotherm and mechanism investigations of the removal of basic violet 3 from water by raw spent coffee grounds. *Physical Chemistry Research* 2020; **8(3)**, 869-884.

[42] OU Trakoolsa and W Yoochatchaval. Adsorption efficiency of copper and nickel by activated carbon from coffee ground. *EnvironmentAsia* 2020; **13(1)**, 46-53.

[43] DW Cho, K Yoon, EE Kwon, JK Biswas and H Song. Fabrication of magnetic biochar as a treatment medium for As (V) via pyrolysis of $FeCl_3$-pretreated spent coffee ground. *Environmental Pollution* 2017; **229**, 942-949.

[44] L Giraldo and JCM Piraján. Synthesis of activated carbon mesoporous from coffee waste and its application in adsorption zinc and mercury ions from aqueous solution. *Journal of Chemistry* 2012; **9(2)**, 938-948.

[45] D Azzouni, EMS Hassani, Z Rais and M Taleb. An excellent alternative to industrial activated carbons for the purification of textile water elaborated from waste coffee grounds. *International Journal of Environmental Research* 2022; **16(5)**, 89.

[46] T Wirawan, S Koesnarpadi and NT Widodo. Study of rhodamine B adsorption onto activated carbon from spent coffee grounds. *AIP Conference Proceedings* 2020; **2237(1)**, 020007.

[47] JW Lim, KY Lam, MJK Bashir, YF Yeong, MK Lam and YC Ho. Spent coffee grounds-based activated carbon preparation for sequestering of malachite green. *AIP Conference Proceedings* 2016; **1787(1)**, 040008.

[48] R Lafi, I Montasser and A Hafiane. Adsorption of congo red dye from aqueous solutions by prepared activated carbon with oxygen-containing functional groups and its regeneration. *Adsorption Science & Technology* 2018; **37(1-2)**, 160-181.

[49] I Loulidi, M Jabri, A Amar, A Kali, A Alrashdi, C Hadey, M Ouchabi, PS Abdullah, H Lgaz, Y Cho and F Boukhlifi. Comparative study on adsorption of crystal violet and chromium (VI) by activated carbon derived from spent coffee grounds. *Applied Sciences* 2023; **13(2)**, 985.

[50] E Pagalan Jr, M Sebron, S Gomez, SJ Salva, R Ampusta, AJ Macarayo, C Joyno, A Ido and R Arazo. Activated carbon from spent coffee grounds as an adsorbent for treatment of water contaminated by aniline yellow dye. *Industrial Crops and Products* 2020; **145(25004)**, 111953.

[51] H Laksaci, A Khelifi, B Belhamdi and M Trari. The use of prepared activated carbon as adsorbent for the removal of orange G from aqueous solution. *Microchemical Journal* 2019; **145**, 908-913.

[52] I Block, C Günter, AD Rodrigues, S Paasch, P Hesemann and A Taubert. Carbon adsorbents from spent coffee for removal of methylene blue and methyl orange from water. *Materials* 2021; **14(14)**, 3996.

[53] VT Nguyen, TB Nguyen, CP Huang, CW Chen, XT Bui and CD Dong. Alkaline modified biochar derived from spent coffee ground for removal of tetracycline from aqueous solutions. *Journal of Water Process Engineering* 2021; **40**, 101908.

[54] M El-Azazy, AS El-Shafie and H Morsy. Biochar of spent coffee grounds as per Se and impregnated with TiO_2: Promising waste-derived adsorbents for Balofloxacin. *Molecules* 2021; **26(8)**, 2295.

[55] A Lykoudi, Z Frontistis, J Vakros, ID Manariotis and D Mantzavinos. Degradation of sulfamethoxazole with persulfate using spent coffee grounds biochar as activator. *Journal of Environmental Management* 2020; **271**, 111022.

[56] A Hgeig, M Novaković and I Mihajlović. Sorption of carbendazim and linuron from aqueous solutions with activated carbon produced from spent coffee grounds: Equilibrium, kinetic and thermodynamic approach. *Journal of Environmental Science and Health, Part B* 2019; **54(4)**, 226-236.

[57] MHL Bergamini, SBD Oliveira and PS Scalize. Production of activated carbon from exhausted coffee grounds chemically modified with natural eucalyptus ash lye and its use in the fluoride adsorption process. *Environmental Science and Pollution Research* 2023; **30(39)**, 91276-91291.

[58] S Zhang, X Huo, S Xu, Y Zhang, B Zhang, M Wang, Q Wang and J. Zhang. Original sulfur-doped carbon materials synthesized by coffee grounds for activating persulfate to BPA degradation: The key role of electron transfer. *Process Safety and Environmental Protection* 2022; **168**, 1219-1234.

[59] N Patel, AL Srivastav, A Patel, A Singh, SK Singh, K Chaudhary, PK Singh and B Bhunia. Nitrate contamination in water resources, human health risks and its remediation through adsorption: A focused review. *Environmental Science and Pollution Research* 2022; **29(4)**, 69137-69152.

[60] MJ Ahmed, BH Hameed and MA Khan. Recent advances on activated carbon-based materials for nitrate adsorption: A review. *Journal of Analytical and Applied Pyrolysis* 2023; **169(7)**, 105856.

[61] H Zhao, H Zhong, Y Jiang, H Li, P Tang, D Li and Y Feng. Porous $ZnCl_2$-activated carbon from shaddock peel: Methylene blue adsorption behavior. *Materials* 2022; **15(3)**, 895.

[62] M Lauberts, I Mierina, M Pals, MAA Latheef and A Shishkin. Spent coffee grounds valorization in biorefinery context to obtain valuable products using different extraction approaches and solvents. *Plants* 2023; **12(1)**, 30.

[63] A Namane, A Mekarzia, K Benrachedi, N Belhaneche-Bensemra and A Hellal. Determination of the adsorption capacity of activated carbon made from coffee grounds by chemical activation with $ZnCl_2$ and H_3PO_4. *Journal of Hazardous Materials* 2005; **119(1-3)**, 189-194.

[64] VT Le, TM Pham, VD Doan, OE Lebedeva and HT Nguyen. Removal of Pb(ii) ions from aqueous solution using a novel composite adsorbent of Fe_3O_4/PVA/spent coffee grounds. *Separation Science and Technology* 2019; **54(18)**, 1-12.

[65] DN Mengesha, MW Abebe, RA Ntiamoah and H Kim. Ground coffee waste-derived carbon for adsorptive removal of caffeine: Effect of surface chemistry and porous structure. *Science of The Total Environment* 2022; **818**, 151669.

[66] LM Madikizela and VE Pakade. Trends in removal of pharmaceuticals in contaminated water using waste coffee and tea-based materials with their derivatives. *Water Environment Research* 2023; **95(4)**, e10857.

[67] VT Le, TKN Tran, NK Dang, VD Doan, VA Tran, Y Vasseghian and TM Aminabhavi. Mn_3O_4/activated carbon nanocomposites for adsorptive removal of methylene blue. *Chemical Engineering Journal* 2023; **474**, 145903.

[68] HM Alraddadi, TM Fagieh, EM Bakhsh, K Akhtar, SB Khan, SA Khan, EA Bahaidarah and TA Homdi. Adsorptive removal of heavy metals and organic dyes by sodium alginate/coffee waste composite hydrogel. *International Journal of Biological Macromolecules* 2023; **274**, 125708.

[69] D Chen, Y Yin, Y Xu and C Liu. Adsorptive recycle of phosphate by MgO-biochar from wastewater: Adsorbent fabrication, adsorption site energy analysis and long-term column experiments. *Journal of Water Process Engineering* 2023; **51**, 103445.

[70] H Laksaci, B Belhamdi, O Khelifi, A Khelifi and M Trari. Elimination of amoxicillin by adsorption on coffee waste based activated carbon. *Journal of Molecular Structure* 2023; **1274(P1)**, 134500.

[71] W Ma, J Fan, X Cui, Y Wang, Y Yan, Z Meng, H Gao, R Lu and W Zhou. Pyrolyzing spent coffee ground to biochar treated with H_3PO_4 for the efficient removal of 2,4-dichlorophenoxyacetic acid herbicide: Adsorptive behaviors and mechanism. *Journal of Environmental Chemical Engineering* 2023; **11(1)**, 109165.

[72] Nurmayasari, SA Kurniasari, S Sholihun and AD Nugraheni. The effectiveness of coffee waste ground by simple washing on the adsorption of methylene blue. *Key Engineering Materials* 2023; **949**, 103-109.

[73] J Wang and X Guo. Adsorption kinetic models: Physical meanings, applications, and solving methods. *Journal of Hazardous Materials* 2020; **390**, 122156.

[74] NNR do Nascimento, ALM da T Silva, WL Silva and MGF Rodrigues. Valorization of coffee agro-industrial residue for biochar production: Use as adsorbent for methylene blue removal. *Desalination and Water Treatment* 2024; **320**, 100767.

[75] DI Çifçi and N Aydın. Comparison of H_3PO_4 and $ZnCl_2$ activated filtered coffee waste carbon-based adsorbents in methylene blue removal by using ultrasonic-assisted adsorption. *Arabian Journal for Science and Engineering* 2023; **48(73)**, 8641-8653.

[76] M Cuccarese, S Brutti, A De Bonis, R Teghil, FD Capua, IM Mancini, S Masi and D Caniani. Sustainable adsorbent material prepared by soft alkaline activation of spent coffee grounds: Characterisation and adsorption mechanism of methylene blue from aqueous solutions. *Sustainability* 2023; **15(3)**, 2454.

[77] MS Akindolie and HJ Choi. Surface modification of spent coffee grounds using phosphoric acid for enhancement of methylene blue adsorption from aqueous solution. *Water Science & Technology* 2022; **85(4)**, 1218-1234.

[78] A Bouzidi, M Djedid, CAdM Benalia, B Hafez and H Elmsellem. Biosorption of Co (II) ions from aqueous solutions using selected local luffa cylindrica: Adsorption and characterization studies. *Moroccan Journal of Chemistry* 2021; **9(1)**, 156-167.

[79] J Hou, C Cao, F Idrees and X Ma. Hierarchical porous nitrogen-doped carbon nanosheets derived from silk for ultrahigh-capacity battery anodes and supercapacitors. *ACS Nano* 2015; **9(3)**, 2556–2564.

[80] N Kumar, A Pandey, Rosy and YC Sharma. A review on sustainable mesoporous activated carbon as adsorbent for efficient removal of hazardous dyes from industrial wastewater. *Journal of Water Process Engineering* 2023; **54**, 104054.

[81] H Zhao, H Zhong, Y Jiang, H Li, P Tang, D Li and Y Feng. Porous $ZnCl_2$-activated carbon from shaddock peel: Methylene blue adsorption behavior. *Materials* 2022; **15(3)**, 895.

[82] A Ahmadpour and DD Do. The preparation of activated carbon from macadamia nutshell by chemical activation. *Carbon* 1997; **32(12)**, 1723-1732.

[83] MA Hubbe, S Azizian and S Douven. Implications of apparent pseudo-second-order adsorption kinetics onto cellulosic materials: A review. *BioResources* 2019; **14(3)**, 7582-7626.

[84] Q Zhang, Y Wu, S Dong, J Zhuo, X Sun, and Q Yao. Development of activated carbon/CaCl2 composites for seasonal thermochemical energy storage: Effect of pore structure. *Journal of Energy Storage* 2024; **97(A)**, 112697.

[85] M Fan, Y. Shao, Y Wang, J Sun, H He, Y Jiang, S Zhang, Y Wang and X Hu. Preparation of activated carbon with recycled $ZnCl_2$ for maximizing utilization efficiency of the activating agent and minimizing generation of liquid waste. *Chemical Engineering Journal* 2024; **500**, 157278.

[86] S Kundu, T Khandaker, MdAM Anik, MdK Hasan, PK Dhar, SK Dutta, MA Latif and MS Hossain. A comprehensive review of enhanced CO_2 capture using activated carbon derived from biomass feedstock. *RSC Advances* 2024; **40(40)**, 29693-29736.

[87] T Fischer, H Kungl, H Tempel, A Kretzschmar, V Selmert and RA Eichelab. Post-treatment strategies for pyrophoric KOH activated carbon

nanofibers. *RSC Advances* 2024; **14(6)**, 3845-3856.

[88] I Pet, MN Sanad, M Farouz, MM ElFaham, AE - Hussein, MSA El-sadek, RA Althobiti, A Ioanid. Review: Recent developments in the implementation of activated carbon as heavy metal removal management. *Water Conservation Science and Engineering* 2024; **9**, 62.

[89] GC Hernández, EP Melián and DE Santiago. Synthesis of activated carbon from sewage sludge using phosphoric acid as activating agent. *Environmental Science and Pollution Research* 2025. https://doi.org/10.1007/s11356-025-36516-y

[90] YAB Neolaka, ZS Ngara, Y Lawa, JN Naat, DP Benu, A Chetouani, H Elmsellem, H Darmokoesoemo and HS Kusuma. Simple design and preliminary evaluation of continuous submerged solid small-scale laboratory photoreactor (CS4PR) using TiO_2/NO_3-@TC for dye degradation. *Journal of Environmental Chemical Engineering* 2019; **7(6)**,103482.

[91] AT Hoang, S Kumar, E Lichtfouse, CK Cheng, RS Varma, N Senthilkumar, PQP Nguyen and XP Nguyen. Remediation of heavy metal polluted waters using activated carbon from lignocellulosic biomass: An update of recent trends. *Chemosphere* 2022; **302**, 134825.